Journal of the European Ceramic Society 17 (1997) 1093–1097

0955-2219/97/$17.00
PII: S0955-2219(96)00210-5

Microstructurally Induced Internal Stresses in β-Si_3N_4 Whisker-Reinforced Si_3N_4 Ceramics

K. Rajan[a] and P. Šajgalík[b]

[a]Rensselaer Polytechnic Institute, School of Engineering, Materials Engineering Department, Troy, New York 12180-3590, USA
[b]Institute of Inorganic Chemistry, Slovak Academy of Sciences, Dúbravská cesta 9, SK-842 36 Bratislava, Slovakia

(Received 27 February 1996; revised version received 10 October 1996; accepted 21 October 1996)

Abstract

The presence of aluminium and oxygen in the outer rim of a whisker, which is grown on the surface of the original β-Si_3N_4 *whisker introduced to the* Si_3N_4 *ceramic prior to hot pressing was observed; it indicates the presence of the* β-*SiAlON phase.*

An estimation of the internal stress generated by whisker impingement in β-Si_3N_4 *whisker-reinforced* Si_3N_4 *composites is reported. The procedure involves the measurement of the angular deviation from the exact Bragg reflection condition, using a transmission electron microscope, associated with lattice bending within* Si_3N_4 *grains when one grain impinges on another. The simple calculations using these results shows that the tensile stress produced on the surface of the impinged whisker as a result of whisker bending is about 340 MPa and the shear stress acting in the area of impingement on the whiskers is substantially higher, 1·4 GPa. This value is comparable to the tensile strength of the silicon nitride whisker. The implications resulting from these microstructural observations on fracture toughness and steric hindrance effects during grain growth are discussed.*
© 1997 Elsevier Science Limited.

Introduction

Silicon nitride-based ceramics/composites are a family of advanced materials that exhibit a combination of high hardness, high strength, good corrosion resistance, high elastic modulus and dimensional stability. In spite of these good properties their wider application in the industry is still restricted by their brittleness, high flaw sensitivity and low reliability. A great effort has been made to improve these last-mentioned properties and quite promising achievements have been reached in this field in recent years. One of the recently most proclaimed ways of improving the properties is the application of the reinforcing filaments in the form of whiskers. The requirement of mechanical and chemical compatibility of the whisker and matrix led workers[1–5] to the application of β-Si_3N_4 whiskers to the Si_3N_4 matrix. Through the application of the β-Si_3N_4 whiskers satisfactory R-curve behaviour and high fracture toughness was achieved.[1–5] The level of improvement of the fracture resistance is proportional, among others, to the volume fraction of the whiskers applied. The amount of whiskers distributed within the matrix should be as high as possible. Much theoretical as well as experimental work to estimate the role of whiskers with respect to the mechanical properties has been done, with the aim of setting the necessary conditions for their maximum efficiency.[6,7,12] The present paper is an attempt to contribute to this effort. The estimation of whisker mechanical behaviour in the matrix is based on direct observations of the microstructure by SEM and TEM. The present paper also shows the possible limitations of this approach. The presence of residual stresses arising from whisker impingement is demonstrated.

Experimental

The β-Si_3N_4–Si_3N_4 composites used for the present study were prepared with Al_2O_3 and Y_2O_3 as the sintering additives by hot pressing at a temperature of 1750°C and pressure of 30 MPa in a static nitrogen atmosphere with overpressure of 30 kPa. The experimental procedure of β-Si_3N_4 whisker addition is described in detail in Refs 4 and 5. Whiskers with mean aspect ratio of ~5 were prepared by SHS method; their characteristics are described in Ref. 8.

The fracture toughness was measured by the indentation method and evaluated by the equation of Shetty *et al.*[9]

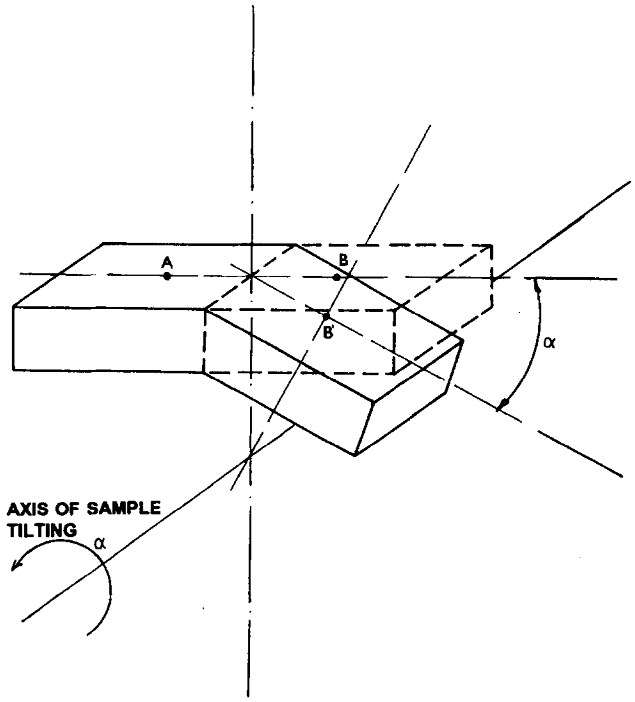

Fig. 1. Measurement of the angle of whisker bending: angle of rotation α is required for spot B' to have the same position as the spot B on the diffraction pattern.

The approach to explore the internal stresses is based on estimating the extent of lattice bending, using what may be described as an electron beam 'rocking curve' experiment. In order to estimate the extent of bending, advantage is taken of the fact that the contrast variations on either side of the grain are associated with local changes in the deviation parameter. The extent of lattice rotation or bending of the grain around the axis normal to the deviation parameter is estimated by sample tilting. The contrast of either side of the whisker was set, spots A and B in the schematic, Fig. 1. Spot B is the projection of the spot B' to the plane of the unbent whisker. Then the sample was tilted till the contrast was the same on the other side, i.e. spot B' reaches the position of spot B, Fig. 1. It is important to recognise that in order to apply this technique meaningfully, it has to be ensured that the bend contour observed in the whisker is

Fig. 2. TEM micrograph of β-Si_3N_4 whisker cross-sections. No. 1 — original β-Si_3N_4 whisker. No. 2 — outer rim grown during the hot pressing containing also aluminium and oxygen.

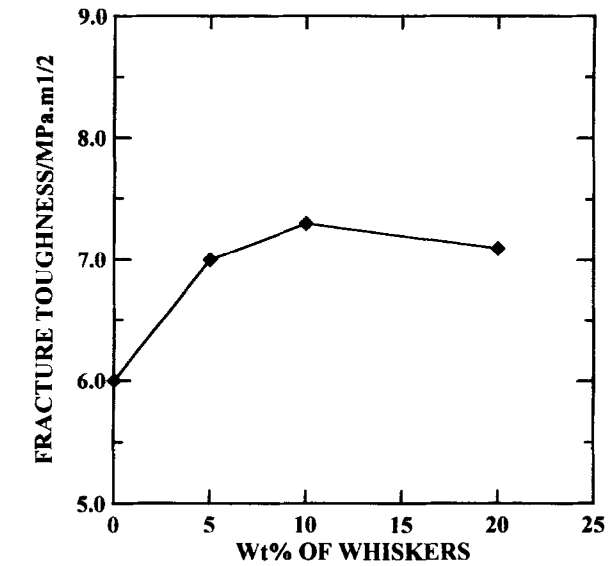

Fig. 3. Fracture toughness versus wt% of whiskers, data from Ref. 4. *Composite, Ref: 4:* Sintering additive 3·4 wt% of Al_2O_3 and 4·6 wt% Y_2O_3, average aspect ratio of β-Si_3N_4 whiskers 5, hot pressing at 1750°C and 30 MPa for 1 h, composite density after hot pressing ≥99% of theoretical.

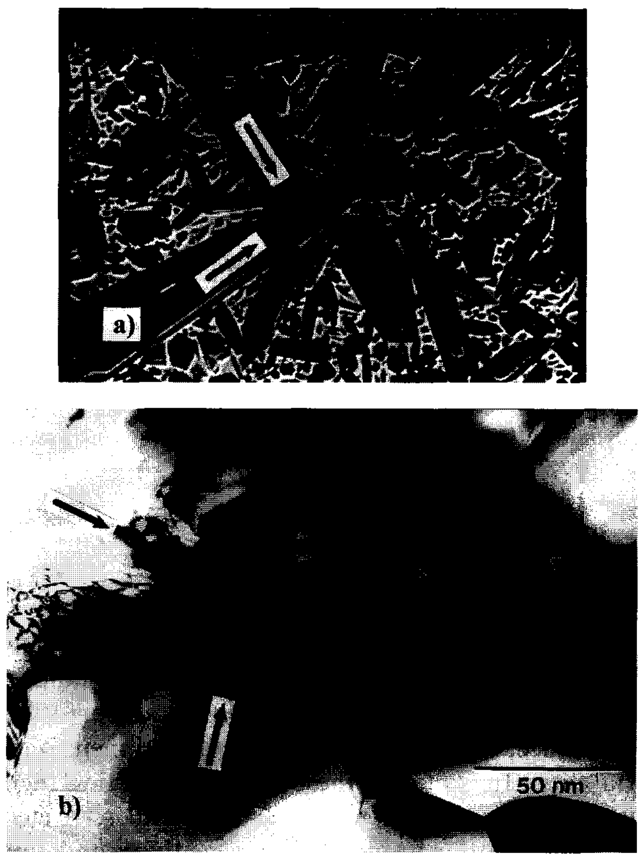

Fig. 4. Microstructure of β-Si_3N_4 whisker-reinforced Si_3N_4 composite. (a) SEM micrograph of plasma etched microstructure, an example of whisker impingement. (b) TEM micrograph of microstructure, the point of whisker impingement with the enhanced dislocation activity area.

not simply due to the bending of the thin foil itself. This was done by detailed examination of the sample, through extensive tilting and dark field observations (which highlighted bend contours which might be missed in a bright field image) to ensure that foil does not have bend contours running through it. In fact, as will be shown below, once the correct experimental precautions were established, one can take advantage of dark field imaging around the region of a local bend contour in the whisker to make estimates of local internal stresses.

Results and Discussion

The detailed study of the microstructure of these composites showed that the β-Si_3N_4 whiskers are grown during the hot pressing process. Figure 2 shows the TEM micrograph of a β-Si_3N_4 whisker cross-section which consists of the core (No. 1 in Fig. 2) and the outer rim (No. 2 in Fig. 2). The outer part is grown during the hot pressing. According to EDX measurements, the core of grain contains the same elements as the outer rim of the grain (nitrogen and silicon) besides aluminium and oxygen which were detected only in the outer part. This indicates that the rim is not pure β-Si_3N_4 but SiAlON. The same result was documented by Krämer and Hoffmann[10,11] for seeds of β-Si_3N_4, which were grown in oxynitride glass containing alumina and yttria. The TEM micrograph shows also the well-developed dislocation pattern on the boundary between the core and the outer rim. This can be explained by different dimensions of the unit cell of SiAlONs and β-Si_3N_4, documented in Ref. 13 and/or by differences in their thermal expansion coefficients.

The dependence of fracture toughness on weight fraction of β-Si_3N_4 whiskers obtained is shown in Fig. 3. A decrease of fracture toughness for β-Si_3N_4 whisker content from 15 to 20 wt% is observed. Similar behaviour of β-Si_3N_4 whisker-reinforced Si_3N_4 ceramics was also observed in Ref. 1. The question of the reason for such a behaviour is still open. For Si_3N_4 ceramics reinforced *in situ* fracture toughness increases with the increase of volume fraction of elongated particles without any minimum, as presented in Ref. 12.

Figure 4(a) shows the microstructure of β-Si_3N_4 whisker-reinforced Si_3N_4 ceramics; an example of impinged β-Si_3N_4 whiskers is presented. Figure 4(b) shows the TEM image of the point of impingement. The exaggerated dislocation activity as a result of impingement is clearly visible. This dislocation pattern can be attributed to the presence of residual stresses. These can possibly arise from two reasons, as a result of firm skeleton formation at a certain volume fraction of applied whiskers, or grain growth during sintering.

The enhanced dislocation activity was mainly observed for the β-Si_3N_4 whisker-reinforced Si_3N_4 ceramics. Microstructural observations of the cracks in these ceramics showed that whiskers are very often broken in the point of impingement in case the crack approaches this point. The restricted number of whiskers taking part in the impingement (total number was five pairs of impinged whiskers) was studied in more details by TEM. Typical behaviour is shown in Fig. 5. Figure 5(a) is a bright field image showing an Si_3N_4 whisker which by the corner of a facet (indicated as No. 1) impinges on another (indicated as No. 2). It is important to note that at the point of impingement, some level of dislocation activity can be observed. Figure 5(b) is a dark field image illuminating only one side of the bend contour, corresponding to the spot A in Fig. 1. In order to estimate the extent of bending, the procedure described in Experimental was employed. The contrast variations on either side of the grain, corresponding to the spots A, B', schematic in Fig. 1, are associated with local changes in the deviation parameter and the extent of the lattice rotation or bending of the whisker around the axis normal to the deviation vector. In this case, it was estimated that the lattice rotation required to shift the illumination in the dark field mode, from one side of the bend contour to the other is approximately 0·5°. This angle was not substantially changed for the other investigated whiskers.

From this value and the schematic shown in Fig. 6 it is possible to estimate the induced stress. The tensile stress σ on the surface of the whisker, Fig. 6, is given as follows:

$$\sigma = E\,(d \sin\alpha / 2L) \qquad (1)$$

where E is the Young's modulus, d is the whisker diameter, L is the whisker length and α is the bending angle. Using the Young's modulus of α-Si_3N_4 whisker as 390 GPa (for β-Si_3N_4 this value is not available)[14] and the average whisker aspect ratio of 5, the tensile stress on the surface of the bent whisker can be estimated, σ = 340 MPa. This value is lower than the whisker strength (for α-Si_3N_4 the reported value is 1·5 GPa),[15] and also microstructural observations did not confirm the enhanced fracture of these slightly bent whiskers.

The calculation of the shear stress can also be done. The bending of whisker No. 1 can be achieved by displacement of whisker No. 2 downwards, Fig. 6. Shear stress acting in the tip of the whisker can be calculated as follows:

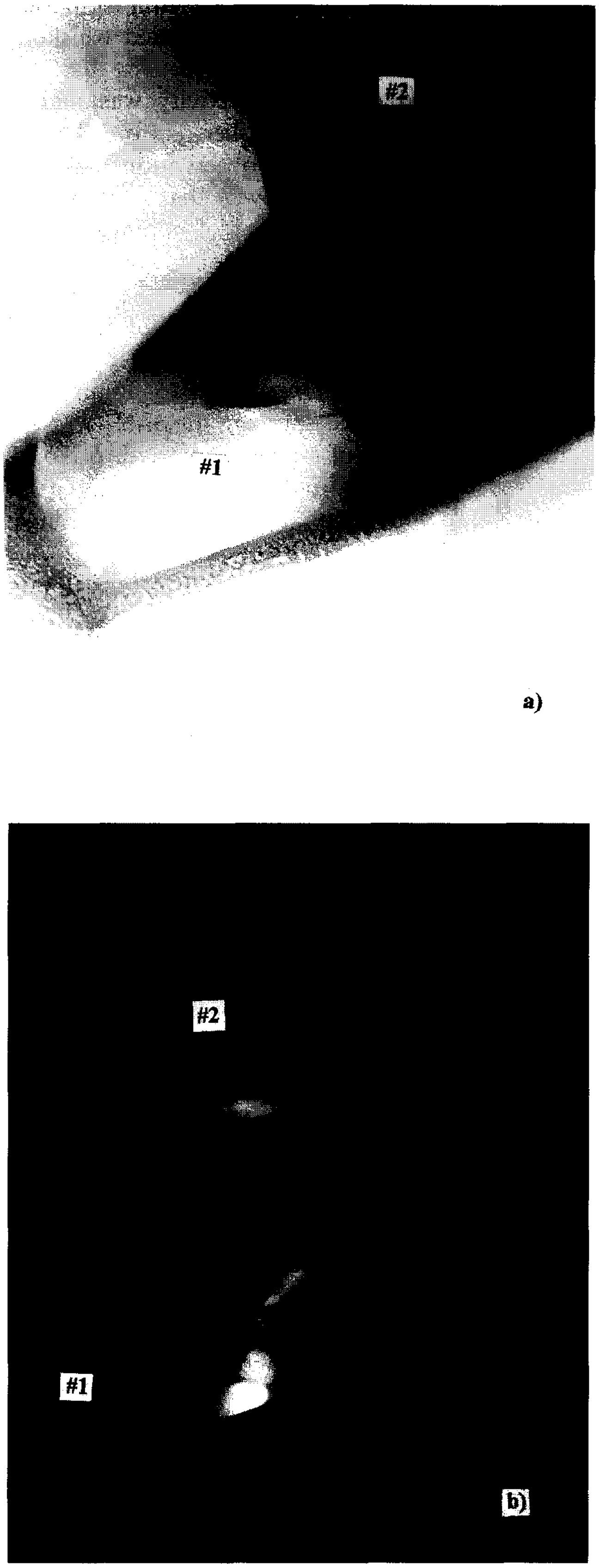

Fig. 5. TEM micrograph of whisker; (a) bright field image, (b) dark field image.

$$\tau = G\alpha = E\alpha/[2(1 + \mu)] \qquad (2)$$

where μ is the Poisson's ratio which is 0·24 for α-Si_3N_4.[14] α is the angle of whisker bending. Using the reported values for E and μ and 0·5° for α, the shear stress calculated from eqn (2) is 1·37 GPa. This value is almost the same as the whisker tensile strength. Based on the action–reaction rule, the same stress is acting in the point of impingement of the adjacent whisker 2, Fig. 6 (this is demonstrated by dislocation area shown in TEM, Fig. 4(b)). This stress seems to be decisive when the propagating crack reaches the point of stress concentration and starts to be opened. At the moment of crack opening, the whisker is loaded in bending, as it was pointed out in Ref. 12. The elasticity of the 'pre-stressed whisker' is substantially lowered and this will be fractured at the stress which is lower as corresponds to its actual strength. An example of such behaviour is in Fig. 7; the propagating crack proceeds along whisker No. 1 and then crosses whisker No. 2 transgranularly at the point of impingement which is supposed to be the region of enhanced dislocation activity as it is shown in Fig. 4(b). The above-mentioned observation can be a base for a hypothesis explaining the fracture toughness decrease at higher volume

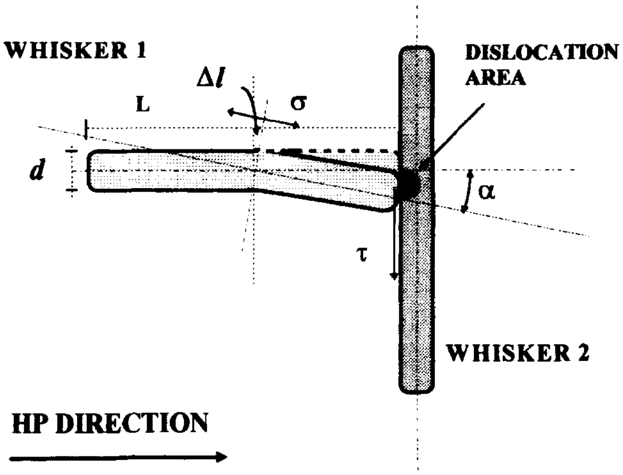

Fig. 6. Schematic of whisker impingement.

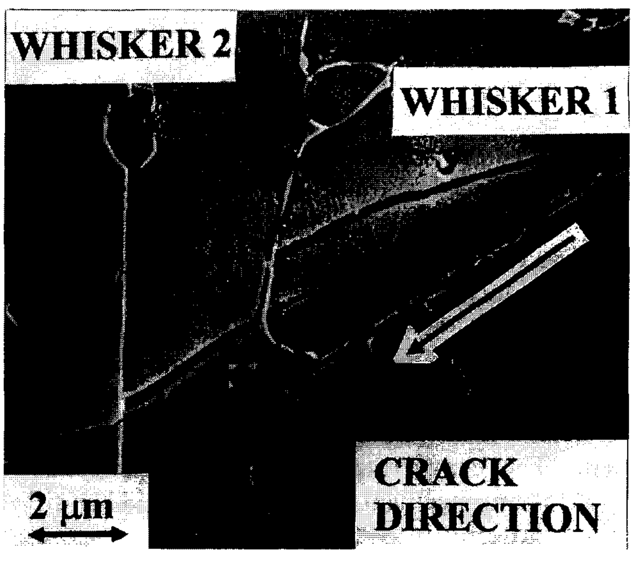

Fig. 7. Whisker failure at the point of whisker impingement.

fractions of β-Si_3N_4 whiskers, Fig. 3. Higher volume fractions of whiskers (>15 wt%) in the composite will enhance this effect because of higher frequency of impingement. Basically it means that the tensile strength of whiskers is changed during the hot pressing or, in other words, the aspect ratio of the whiskers is decreased by presence of stresses which allows the whisker to fail by cracking. In fact, the actual whisker length in the hot pressed body (for the high volume fraction of β-Si_3N_4 whiskers >15 wt%) is thus different compared to its original length introduced into the starting mixture. In these cases (volume fraction of β-Si_3N_4 whiskers >15 wt%) the microstructure loses its former ability to resist the propagating crack by toughening mechanisms resulting from the presence of high-aspect-ratio whiskers.

Conclusions

β-Si_3N_4 whiskers introduced into the starting powder mixture containing alumina and yttria as sintering additives are grown during the green body densification by hot pressing. The grown phase contains also oxygen and aluminium, the contents of which are stepwise changed at the subgrain boundary splitting the original β-Si_3N_4 whisker and new grown phase from the liquid. This observation implies that SiAlON is formed when alumina is used as one of the sintering additives.

Enhanced dislocation activity in the point of whisker impingement was observed; the whisker failure within this stress area was also documented. Based on these observations the hypothesis that these stresses are responsible for the whisker weakening and so the degradation of fracture toughness of β-Si_3N_4 whisker-reinforced Si_3N_4 composites with higher volume fraction of β-Si_3N_4 whiskers was drawn.

Acknowledgements

This work was supported by the Agency for International Scientific and Technological Cooperation, US–Slovak Science and Technology Program, grant 940 39 and partially by Slovak Grant Agency, grant 2/1169/95.

References

1. Chu, C.-Y. and Shing, J. P., Mechanical properties and microstructure of Si_3N_4-whisker reinforced Si_3N_4 matrix composites. *Ceram. Engng. Sci. Proc.*, 1990, **11**(7–8), 709–720.
2. Homeny, J. and Neergaard, L. J., Mechanical properties of β-Si_3N_4-whisker/Si_3N_4-matrix composites. *J. Am. Ceram. Soc.*, 1990, **73**(11), 3493–3496.
3. Hirao, K., Nagaoka, T., Brito, M. E. and Kanazaki, S., Microstructure control of silicon nitride by seeding with rodlike β-silicon nitride particles. *J. Am. Ceram. Soc.*, 1994, **77**(7), 1857–1862.
4. Šajgalík, P. and Dusza, J., Reinforcement of silicon nitride ceramics by β-Si_3N_4 whiskers *J. Eur. Ceram. Soc.*, 1989, **5**, 321–326.
5. Šajgalík, P. and Dusza, J., Development of β-Si_3N_4-reinforced ceramics. In *Euro-ceramics* II, Vol. 2, ed. G. Ziegler and H. Hausner, DKG e.V., 1993, pp. 1589–1593.
6. Becher, P. F., Microstructural design of toughened ceramics. *J. Am. Ceram. Soc.*, 1991, **74**(2), 222–269.
7. Bengisu, M., Intal, O. T. and Tosiali, O., On whisker toughening in ceramic materials. *Acta. Metall. Mater.*, 1991, **39**(11), 2509–2517.
8. Dusza, J., Šajgalík, P., Bastl, Z., Kavečanský, V. and Ďurišin, J., Properties of β-silicon nitride whiskers. *J. Mater. Sci. Lett.*, 1992, **11**, 208–211.
9. Shetty, D. K., Wright, I. G., Mincer, P. N. and Clauer, A. H., Indentation fracture of WC-Co cermets. *J. Mater. Sci.*, 1985, **20**, 1873–1882.
10. Krämer, M., Hoffmann, M. J. and Petzow, G., Grain growth studies of silicon nitride dispersed in an oxynitride glass. *J. Am. Ceram. Soc.*, 1993, **76**(11), 2778–2784.
11. Hoffmann, M. J., Analysis of microstructural development and mechanical properties of Si_3N_4 ceramics. In *Tailoring of Mechanical Properties of Si_3N_4 Ceramics.* NATO ASI Series, Series E: *Applied Sciences*, Vol. 276, ed. M. J. Hoffmann and G. Petzow. Kluwer Academic Publishers, Dordrecht, 1994, pp. 59–72.
12. Šajgalík, P., Dusza, J. and Hoffman, M. J., Relationship between microstructure, toughening mechanisms, and fracture toughness of reinforced silicon nitride ceramics. *J. Am. Ceram. Soc.*, 1995, **78**(10), 2619–2624.
13. Haviar, M. and Johannesen, O., Unit-cell dimensions of β'-sialons. *Advanced Ceramic Materials*, 1988, **3**(4), 405–407.
14. Becher, P. F. and Tiegs, T. N., Whisker-reinforced ceramics. In *Engineered Materials Handbook*, Vol. 1, *Composites*. ASM International, USA, 1987, pp. 941–944.
15. Hampshire, S., Engineering properties of nitrides. In *Engineered Materials Handbook*, Vol. 4, *Ceramics and Glasses*, ed. S. J. Schneider, Jr. ASM International, USA, 1991, pp. 812–820.